Theor Chem Acc (2012) 131:1114
DOI 10.1007/s00214-012-1114-1

REGULAR ARTICLE

Halogen bonding and beyond: factors influencing the nature of CN–R and SiN–R complexes with F–Cl and Cl_2

Peter Politzer · Jane S. Murray

Received: 3 October 2011 / Accepted: 7 November 2011 / Published online: 9 February 2012

Abstract It was recently shown that complexes of the type F–Cl···CN–R, ostensibly halogen bonded, sometimes have properties (relatively high binding energies, short Cl–C separations and considerably lengthened F–Cl distances) that are inconsistent with typical halogen bonds (Del Bene et al. in J Phys Chem A 114:12958–12962, 2010). We attribute these anomalous features, as well as analogous observations for F–Cl···SiN–R systems, to the strong polarization of the CN–R carbons and SiN–R silicons by the electric field of the positive σ-hole of the F–Cl chlorine. This polarization may evolve into some degree of dative sharing of electrons by the carbons and silicons. This interpretation is supported by the fact that complexes of CN–R and SiN–R with Cl–Cl, which has a much weaker positive σ-hole than F–Cl, are considerably less likely to show the unusual features. It is demonstrated that the full ranges of binding energies of the CN–R and SiN–R complexes with either F–Cl or Cl–Cl can be represented well ($R^2 > 0.96$) in terms of the most negative electrostatic potentials and the lowest local ionization energies on the carbon and silicon surfaces. These properties reflect the electrostatic components of the interactions and the polarizabilities/dative reactivities of the carbons and silicons.

Keywords Halogen bonding · Local ionization energies · Electrostatic potentials · Dative bonding · Polarization

P. Politzer · J. S. Murray (✉)
CleveTheoComp, 1951 W. 26th Street,
Suite 409, Cleveland, OH 44113, USA
e-mail: jsmurray@uno.edu

1 Halogen bonding

It was discovered in 1992 [1], and subsequently confirmed [2, 3], that covalently bonded halogen atoms may have regions of positive electrostatic potential on their outer portions, along the extensions of the covalent bonds (Fig. 1). These regions arise from the anisotropies of the bonded halogens' charge distributions [4–10]. The electronic density on the side of the halogen opposite to the bond is somewhat diminished, creating a so-called σ-hole [11]. If the electronic density is sufficiently reduced, then a positive potential develops in the σ-hole [12]. Through such a positive σ-hole, a halide R–X (X = halogen) can interact electrostatically, in a highly directional manner, with a negative site such as a Lewis base B. In the resulting complex R–X–B, the angle R–X–B is very close to 180°, barring secondary effects. The separation X–B is normally less than the sum of the respective van der Waals radii. This is called halogen bonding [3, 12–15]; R–X and B are labeled the halogen bond donor and acceptor, respectively.

The existence of such interactions is well established experimentally, for example through infrared analyses of halide solutions [16, 17] and extensive surveys of crystallographic close contacts [3, 18–20]. Computationally, correlations have been observed, within given structural frameworks, between the strengths of halogen bonds and the magnitudes of the positive σ-hole potentials [21–23]. This demonstrates the key role of electrostatics in the interactions.

The σ-hole potential depends largely upon two factors: It increases (a) as the R portion of the halide R–X becomes more electron-withdrawing, and (b) in going from the lighter to the heavier halogens, which are more polarizable and less electronegative [12, 14]. Covalently bonded fluorine, the least polarizable and most electronegative

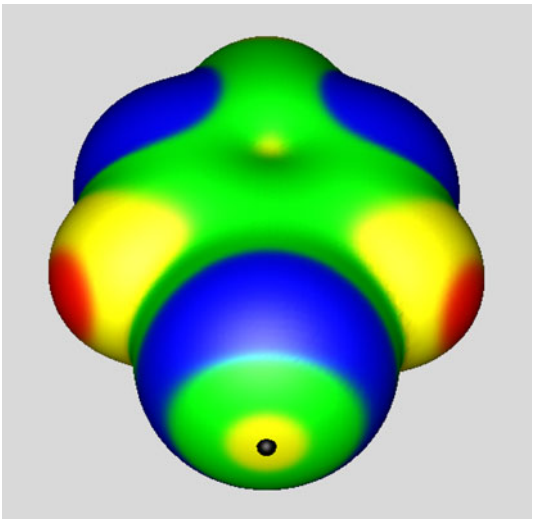

Fig. 1 Computed electrostatic potential on the 0.001 au molecular surface of *meta*-chloropyrimidine. The chlorine is in the foreground; the nitrogens are in the back. Color ranges, in kcal/mol, are as follows: *red* greater than 20; *yellow* from 10 to 20; *green* from 0 to 10; *blue* less than 0 (*negative*). The position of the $V_{S,\max}$ on the chlorine is denoted by a *black* hemisphere; its value is 13.3 kcal/mol

halogen, is often insufficiently anisotropic to have a positive σ-hole; halogen bonding by fluorides is accordingly less common, but certainly not nonexistent [12, 24–26].

It should be noted that, unless the remainder of the molecule is extremely electron-withdrawing, a positive σ-hole on a covalently bonded halogen is generally surrounded by negative potential. This can be seen in Fig. 1. This means, as was pointed out by Brinck et al. already in 1993 [2], that the atom can interact electrostatically with both nucleophilic and electrophilic sites [12, 27–29]. This explains earlier observations of close contacts in crystalline halides [18–20].

We have described halogen bonding as electrostatically driven. However, it must be recognized that the formation of a complex R–X···B also involves mutual polarization [12, 30]. The electric field of R–X, which reflects the positive σ-hole on X, polarizes the electronic charge of B, while the electric field of B in turn polarizes R–X. In terms of the latter, effect can be explained the red-shifting or blue-shifting of the R–X bond [31–34]. There is evidence that if the electric field due to the negative site is sufficiently strong, then it can actually induce a positive σ-hole [12]. Finally, there is also a dispersion contribution to halogen bonding [21].

2 Halogen bonding and beyond

A halogen bond, R–X···B, typically satisfies several criteria: (a) The angle R–X–B is near 180°, unless there are significant secondary interactions [26]. (b) The binding energy, for neutral B, is less than about 8 kcal/mol [12]. (c) The R–X bond in the complex may be longer or shorter than in the free R–X molecule, but usually by no more than 0.03 Å [33, 34]. (d) The X–B separation is generally 5–30% less than the sum of the respective van der Waals radii [12].

However, a recent computational study of some ostensibly halogen-bonded complexes, by Del Bene et al. [35], found some very striking deviations from these criteria. They investigated a series of complexes of the type F–Cl···CN–R, in which R ranged from strongly electron-withdrawing (R=CN, NO_2) to strongly electron-donating (R = Li, Na). Formally, these can be viewed as examples of halogen bonding, with the carbon of CN–R being the negative site. The key computed properties of these complexes—the F–Cl and Cl–C distances and the binding energies BE—are given in Table 1. They were obtained with the MP2/aug'-cc-pVTZ procedure [35]. The binding energies are defined as

$$\mathrm{BE} = \mathrm{E(F{-}Cl)} + \mathrm{E(CN{-}R)} - \mathrm{E(F{-}Cl\cdots CN{-}R)} \qquad (1)$$

using the respective minimum energies at 0 K.

All of the complexes were found to have F–Cl–C angles of 180°, thus satisfying the linearity criterion. The first four have BE < 8 kcal/mol and Cl–C separations of 2.4–2.5 Å, about 70% of the sum of the chlorine and carbon van der Waals radii (3.46 Å [36]). The F–Cl bond lengths in these four systems are about 1.67 Å, just a little longer than the computed 1.639 Å in free F–Cl. This is all as expected for halogen bonding.

Starting with F–Cl···CN–CF_3, however, there is a dramatic increase in the strengths of the interactions as R becomes more electron-donating and the carbon of CN–R correspondingly more negative. The Cl–C separation decreases markedly, to roughly 1.70 Å for the remaining systems. This is less than half of the sum of the chlorine and carbon van der Waals radii; it is in fact nearly equal to the crystallographic Cl–C(*sp*) bond length, approximately 1.64 Å [37]. Meanwhile the F–Cl bond stretches sharply to about 1.86 Å, and then gradually lengthens to 2.003 Å. Finally, the binding energy increases remarkably, to 33.4 kcal/mol for F–Cl–CN–Na! Del Bene et al. interpreted their results as indicating that the interactions are changing from "traditional" halogen bonding to chlorine-shared and, in the case of the CN–Li and CN–Na complexes, ion-pair halogen bonds.

It is certainly evident that many of the interactions in Table 1 are beyond what is normally viewed as halogen bonding. In this context, it may be relevant that F–Cl possesses the most positive chlorine σ-hole that we have encountered, reaching a maximum of 39.9 kcal/mol at the B3PW91/6-31G(d,p) level (Fig. 2). This should exert a rather strongly polarizing electric field upon the CN–R carbons and perhaps induce a degree of dative (coordinate

Table 1 Computed properties for F–Cl···CN–R complexes

Complex	Properties of complex[a]			Properties of free CN–R[b]	
	R(F–Cl)[c]	R(Cl–C)[d]	BE	$V_{S,\min}$	$\bar{I}_{S,\min}$
F–Cl···CN–CN	1.666	2.467	5.48	−17.2	10.17
F–Cl···CN–NC	1.668	2.448	5.88	−21.3	9.89
F–Cl···CN–NO_2	1.674	2.411	5.97	−19.1	10.02
F–Cl···CN–F	1.670	2.454	6.18	−25.7	9.58
F–Cl···CN–CF_3	1.864	1.696	8.27	−24.4	9.56
F–Cl···CN–Cl	1.854	1.749	8.97	−28.3	9.24
F–Cl···CN–Br	1.867	1.731	10.78	−29.4	9.15
F–Cl···CN–H	1.875	1.712	10.86	−34.2	8.74
F–Cl···CN–CCF	1.877	1.700	11.63	−30.8	9.08
F–Cl···CN–CCH	1.878	1.693	11.64	−29.9	9.17
F–Cl···CN–CH_3	1.888	1.724	14.13	−39.5	8.25
F–Cl···CN–SiH_3	1.903	1.684	15.45	−34.3	8.64
F–Cl···CN–Li	1.976	1.684	28.94	−59.1	6.62
F–Cl···CN–Na	2.003	1.684	33.40	−65.3	6.10

[a] R(F–Cl) and R(Cl–C) are distances in Å; BE is binding energy in kcal/mol. Computational level: MP2/aug'-cc-pVTZ. Data taken from reference [35]

[b] $V_{S,\min}$, in kcal/mol, and $\bar{I}_{S,\min}$, in eV, both refer to the carbons of the CN–R. The positions of the $V_{S,\min}$ and the $\bar{I}_{S,\min}$ coincide; they are on the extensions of the N–C bonds. Computational level: B3PW91/6-31G(d,p)

[c] Computed bond length in free F–Cl is 1.639 Å

[d] Sum of chlorine and carbon van der Waals radii is 3.46 Å [36]

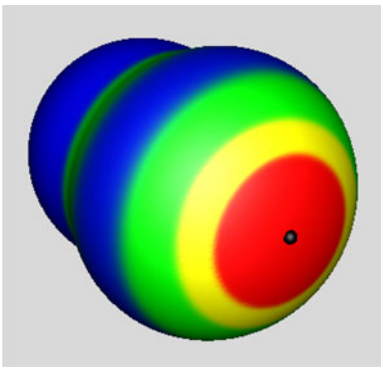

Fig. 2 Computed electrostatic potential on the 0.001 au molecular surface of F–Cl. The chlorine is in the foreground. Color ranges, in kcal/mol, are as follows: *red* greater than 20; *yellow* from 10 to 20; *green* from 0 to 10; *blue* less than 0 (negative). The position of the $V_{S,\max}$ on the chlorine is denoted by a *black* hemisphere; its value is 39.9 kcal/mol

covalent) character involving some sharing of their lone pair electrons. This has already been invoked qualitatively in earlier analyses of gradations in intermolecular interactions [38, 39].

Our objective in this work has been to try to rationalize quantitatively the variations in the strength of binding in the complexes in Table 1. Since both electrostatic and polarization/dative factors may be involved, we shall focus upon two relevant properties, the electrostatic potential and the average local ionization energy. These properties shall be briefly reviewed in the next two sections. We shall also look at the effect of the halogen bond donor.

3 The electrostatic potential

The nuclei and electrons of a molecule produce an electrostatic (Coulomb) potential $V(\mathbf{r})$ at any point $\mathbf{r}$ in the space of a molecule. Its value is given by

$$V(\mathbf{r}) = \sum_A \frac{Z_A}{|\mathbf{R}_A - \mathbf{r}|} - \int \frac{\rho(\mathbf{r}')d\mathbf{r}'}{|\mathbf{r}' - \mathbf{r}|} \quad (2)$$

where Z_A is the charge on nucleus A, located at $\mathbf{R}_A$, and $\rho(\mathbf{r})$ is the molecule's electronic density.

$V(\mathbf{r})$ is a physical observable; it can be obtained experimentally, using diffraction methods [40, 41], as well as computationally. The sign in any region depends upon whether the positive contribution of the nuclei or the negative one of the electrons is dominant there.

The electrostatic potential is a fundamental molecular property [42], which has been shown to be an effective guide to interpreting and predicting noncovalent reactive behavior. For example, a number of condensed phase physical properties that depend upon noncovalent interactions can be expressed analytically in terms of the quantitative features of $V(\mathbf{r})$ [42–44].

For such purposes, $V(\mathbf{r})$ is usually computed and analyzed on the molecule "surface," which is commonly taken to be the 0.001 au (electrons/bohr^3) contour of the electronic density, as proposed by Bader et al. [45]. Defining the surface as an outer contour of $\rho(\mathbf{r})$ has the advantage of being specific to the particular molecule, that is, reflecting its lone pairs, π electrons, strained bonds, atomic anisotropies, etc. $V(\mathbf{r})$ calculated on the molecular surface is labeled $V_S(\mathbf{r})$; its locally most positive and most negative values, of which there may be several, are designated as the $V_{S,\max}$ and $V_{S,\min}$, respectively. Thus, positive σ-holes are typically characterized by $V_{S,\max}$, which are normally located along the extensions of the R–X bonds (see Figs. 1, 2).

4 The average local ionization energy

A quantitative indicator of the polarizability/reactivity of the electronic charge in a molecule, on a local level, is the average local ionization energy, $\bar{I}(\mathbf{r})$. It was introduced within the framework of Hartree–Fock theory as [46]

$$\bar{I}(\mathbf{r}) = \frac{\sum_i \rho_i(\mathbf{r})|\varepsilon_i|}{\rho(\mathbf{r})} \tag{3}$$

In Eq. 2, $\rho_i(\mathbf{r})$ is the electronic density of orbital i at the point $\mathbf{r}$, ε_i is the orbital's energy, and $\rho(\mathbf{r})$ is the molecular electronic density. The summation is over all occupied orbitals.

$\bar{I}(\mathbf{r})$ is viewed as the energy needed for removal of an electron at $\mathbf{r}$, focusing upon the point in space rather than a particular orbital. This interpretation is based upon the Hartree–Fock formalism [47], with some support from Koopmans' theorem [48, 49]. However, $\bar{I}(\mathbf{r})$ as given by Eq. 2 has also been found to be effective within the framework of Kohn–Sham density functional theory [47, 50, 51]; the magnitudes are different but the trends are generally the same.

$\bar{I}(\mathbf{r})$ has been used successfully to analyze and predict various aspects of molecular reactivity [47, 52]. For such applications, it is computed on the 0.001 au molecular surface and denoted $\bar{I}_S(\mathbf{r})$. Of particular interest are the points where $\bar{I}_S(\mathbf{r})$ has its minimum values, $\bar{I}_{S,\min}$. These indicate the locations of the least tightly held, most reactive and polarizable electrons. The $\bar{I}_{S,\min}$ have been shown to correctly describe the directing tendencies and ring activation and deactivation of benzene substituents, to identify radical sites and strained bonds, to correlate with pK_a, etc. For a recent review, see Politzer et al. [47].

What is particularly relevant to our present interests is that $\bar{I}_S(\mathbf{r})$ has been related inversely to local polarizability [47, 53]. This follows from the fact that it is the least tightly held electrons that are the most affected by an electric field (i.e., are the most polarizable) [54, 55].

5 $V_S(\mathbf{r})$ and $\bar{I}_S(\mathbf{r})$ relationships

The halogen bond donor in all of the systems in Table 1 is F–Cl. Accordingly, it is presumably the properties of the CN–R carbons that determine the variations in structures and binding energies of the resulting complexes. We will focus in particular upon (a) the most negative electrostatic potential ($V_{S,\min}$) on the surfaces of the carbons, since these are what interacts with the chlorine σ-hole, and (b) the lowest local ionization energies ($\bar{I}_{S,\min}$) on the carbons, as an inverse measure of the polarizabilities and availabilities for dative sharing of their lone pairs.

We have computed the $V_{S,\min}$ and $\bar{I}_{S,\min}$ on the 0.001 au surfaces of the carbons in the *free* CN–R molecules (Table 1). (We need the $V_{S,\min}$ and $\bar{I}_{S,\min}$ *prior* to interaction, since these are what governs it.) Gaussian 09 [56] was used at the B3PW91/6-31G(d,p) level to obtain the wave functions and the Wave Function Analysis–Surface Analysis Suite [57] for $V_S(\mathbf{r})$ and $\bar{I}_S(\mathbf{r})$.

An interesting feature of an atom that is in the same valence state (i.e., orbital configuration) in a series of different molecules is that its $V_{S,\min}$ and $\bar{I}_{S,\min}$ in those molecules correlate extremely well with each other. This may seem surprising, because $V_{S,\min}$ and $\bar{I}_{S,\min}$ are viewed as quite different properties. It can be rationalized by noting that as a site becomes more negative (positive), its electrons should be less (more) strongly bound and $\bar{I}_S(\mathbf{r})$ should decrease (increase). Thus, direct correlations were found between the lone pair $V_{S,\min}$ and $\bar{I}_{S,\min}$ of the nitrogen's in substituted anilines [60, 61] and the hydroxyl oxygens in substituted phenols and benzoic acids [62]. Such correlations do not in general exist, however, between different atoms or different valence states. (For a discussion of fundamental relationships between $\bar{I}(\mathbf{r})$ and $V(\mathbf{r})$, see Politzer et al. [47]).

Figure 3 is a plot of $\bar{I}_{S,\min}$ versus $V_{S,\min}$ for the carbons of the free CN–R molecules (Table 1). The carbon is in the same valence state in all of them. We obtain a nearly perfect linear relationship between $\bar{I}_{S,\min}$ and $V_{S,\min}$. The R^2 value is 0.999 and the F ratio is 8294. (R^2 is the proportion of the variation in $\bar{I}_{S,\min}$ that is due to the variation in $V_{S,\min}$; F is the ratio of the weighted explained and unexplained variations.) $\bar{I}_{S,\min}$ decreases in direct proportion to $V_{S,\min}$ becoming more negative.

6 Binding energies of complexes

6.1 F–Cl···CN–R

While Table 1 shows notable and sometimes very abrupt variations in the F–Cl and Cl–C distances as well as in the

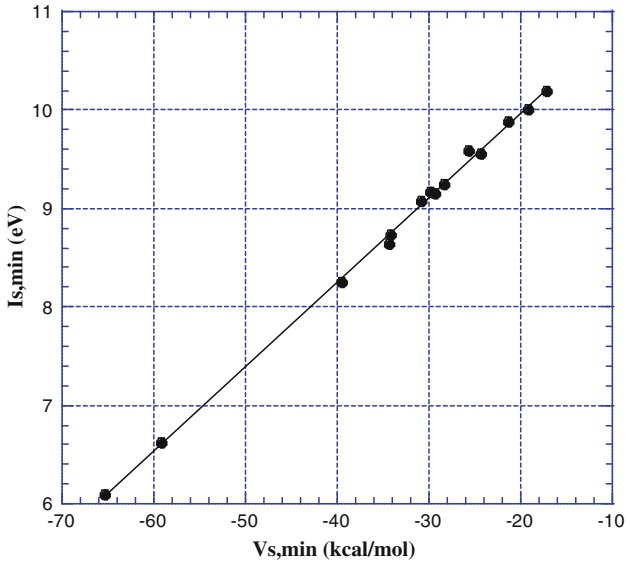

Fig. 3 Plot of carbon $\bar{I}_{S,min}$ versus $V_{S,min}$ for the fourteen CN–R molecules in Table 1

binding energies, it is the latter that we will try to rationalize in terms of the $\bar{I}_{S,min}$ and/or the $V_{S,min}$ of the CN–R carbons. We use the NCSS code to obtain either one- or two-variable regressions [63].

In view of the very close correlation between the carbon $\bar{I}_{S,min}$ and $V_{S,min}$ (Fig. 3), seeking a double regression is not warranted; if BE can be related to either $\bar{I}_{S,min}$ or $V_{S,min}$ alone, then it should be essentially equally well related to the other, and using both would lead to no significant improvement. This is indeed the case. As summarized in Table 2, both BE $\sim \bar{I}_{S,min}$ and BE $\sim V_{S,min}$ have $R^2 \geq 0.970$, root-mean-square (RMS) error $\leq$1.5 kcal/mol and $F > 390$. A double regression, expressing BE as a function of both $\bar{I}_{S,min}$ and $V_{S,min}$, has $R^2 = 0.981$, RMS error = 1.25 kcal/mol and $F = 283$.

It is gratifying that these simple relationships are able to reproduce the striking variation in the computed BE of the F–Cl···CN–R complexes (Table 1). However, the close correlation between the carbon $\bar{I}_{S,min}$ and $V_{S,min}$ makes it difficult to assess their relative roles and to determine whether both of them will sometimes be needed. We decided, therefore, to expand our study.

6.2 F–Cl···CN–R and F–Cl···SiN–R

In Table 3 are listed the computed properties of eight F–Cl···SiN–R complexes. These are analogues of eight of those in Table 1, with silicon having replaced carbon as the site interacting with the chlorine σ-hole. The calculations were at the same levels as for Table 1.

The F–Cl–Si angles in all of the systems in Table 3 are 180°. However, only the first, F–Cl···SiN–F, meets the other three criteria for halogen bonding. Starting with the second, F–Cl···SiN–Cl, the F–Cl distances are much longer than the bond length of free F–Cl while the Cl–Si separations are little more than half of the sum of the chlorine and silicon van der Waals radii (3.9 Å [36]); in fact, they approach the computed MP2/aug'-cc-pVTZ length of the Cl–Si bond in Cl–Si≡N, 2.038 Å. The BE increase slowly, only those for SiN–Li and SiN–Na being high. The latter two molecules have by far the most negative $V_{S,min}$ and lowest $\bar{I}_{S,min}$, as did their CN-R counterparts (Table 1); these features can be expected to greatly promote interactions.

Since the silicons in the SiN-R molecules are all in the same valence state, it can be anticipated that their $\bar{I}_{S,min}$ and $V_{S,min}$ will correlate. This was confirmed (Fig. 4); R^2 is 0.978 and the F ratio is 267. However, since carbon and silicon are different atoms, the respective $\bar{I}_{S,min}$ versus $V_{S,min}$ plots do not coincide. Instead they are nearly parallel, with slopes of 0.0857 (CN–R molecules) and 0.0626 (SiN–R molecules; Fig. 4). The separation between the two lines, as measured by the difference in their intercepts, is 3.3 eV, which is similar to the difference between the first ionization energies of free carbon and silicon atoms, 3.1 eV [64].

It should not be expected that the BE of the twenty-two F–Cl···CN–R and F–Cl···SiN–R systems, taken together, will correlate with just the $V_{S,min}$ of the carbons and silicons or just their $\bar{I}_{S,min}$, since the $\bar{I}_{S,min}$ and $V_{S,min}$ do not correlate with each other (Fig. 4). The key question then becomes: Can the BE of all twenty-two F–Cl···CN–R and

Table 2 Binding energy relationships

Complexes	Regression equation	R^2	RMS error[a]	F ratio
F–Cl···CN–R	BE = −7.045 ($\bar{I}_{S,min}$) + 75.40	0.978	1.30	527
F–Cl···CN–R	BE = −0.598 ($V_{S,min}$) − 6.74	0.970	1.51	391
F–Cl···CNR, SiN–R	BE = −4.018 ($\bar{I}_{S,min}$) − 0.2768 ($V_{S,min}$) + 39.56	0.987	1.02	693
Cl–Cl···CNR, SiN–R	BE = −2.985 ($\bar{I}_{S,min}$) − 0.1143 ($V_{S,min}$) + 27.63	0.961	0.99	87

BE and $V_{S,min}$ are in kcal/mol; $\bar{I}_{S,min}$ is in eV

[a] Root-mean-square error, in kcal/mol

Table 3 Computed properties for F–Cl···SiN–R complexes

Complex	Properties of complex[a]			Properties of free SiN–R[b]	
	R(F–Cl)[c]	R(Cl–Si)[d]	BE	$V_{S,\min}$	$\bar{I}_{S,\min}$
F–Cl···SiN–F	1.654	2.939	1.90	7.0	8.71
F–Cl···SiN–Cl	1.804	2.226	3.42	5.0	8.64
F–Cl···SiN–CCH	1.820	2.191	4.09	4.3	8.58
F–Cl···SiN–CCF	1.829	2.178	4.21	3.4	8.50
F–Cl···SiN–H	1.837	2.173	6.61	−2.9	8.49
F–Cl···SiN–CH_3	1.861	2.156	7.77	−6.0	8.14
F–C···SiN–Li	1.928	2.121	20.60	−26.3	6.72
F–Cl···SiN–Na	1.951	2.119	23.93	−32.1	6.28

[a] R(F–Cl) and R(Cl–Si) are distances in Å; BE is binding energy in kcal/mol. Computational level: MP2/aug'-cc-pVTZ

[b] $V_{S,\min}$, in kcal/mol, and $\bar{I}_{S,\min}$, in eV, both refer to the silicons of the SiN–R. The positions of the $V_{S,\min}$ are along the extensions of the N–Si bonds, while the $\bar{I}_{S,\min}$ form rings around the sides of the silicon atoms (except for R = Li, in which case the positions of $V_{S,\min}$ and $\bar{I}_{S,\min}$ coincide). Computational level: B3PW91/6-31G(d,p)

[c] Computed bond length in free F–Cl is 1.639 Å

[d] Sum of chlorine and silicon van der Waals radii is 3.9 Å [36]

F–Cl···SiN–R complexes be represented by the double regression Eq. 4, in terms of the $\bar{I}_{S,\min}$ and $V_{S,\min}$ of all of the CN–R and SiN–R molecules?

$$\mathrm{BE} = \alpha \bar{I}_{S,\min} + \beta V_{S,\min} + \gamma \quad (4)$$

Figure 5 answers this affirmatively; $R^2 = 0.987$, the RMS error is 1.02 kcal/mol and $F = 693$ (Table 2). Figure 5 demonstrates unequivocally the complementary roles of $\bar{I}_{S,\min}$ and $V_{S,\min}$ in accounting for the variations in the binding energies of the F–Cl complexes.

6.3 Cl–Cl complexes with both CN–R and SiN–R molecules

In all of the interactions that have been considered (Tables 1, 3), the positive σ-hole has been that of the chlorine in F–Cl; this has been a constant factor, while the nature of the base changed. As was mentioned earlier, the chlorine in F–Cl has a relatively strongly positive σ-hole, with $V_{S,\max} = 39.9$ kcal/mol. In order to see the effects of a weaker but still positive σ-hole, we repeated the computational analysis for a

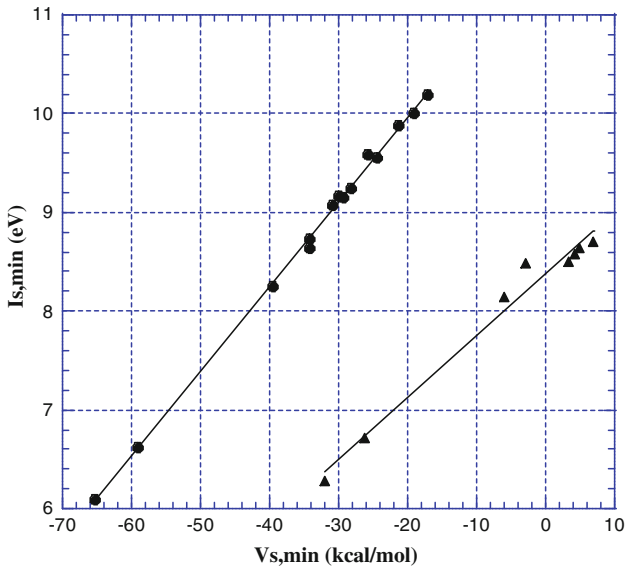

Fig. 4 Plot of carbon and silicon $\bar{I}_{S,\min}$ versus $V_{S,\min}$ for the fourteen CN–R (*circles*) and the eight SiN–R (*triangles*) molecules in Tables 1 and 3

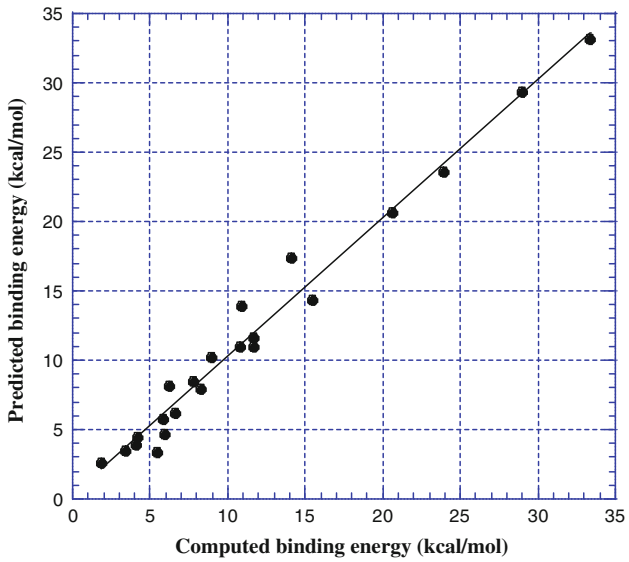

Fig. 5 Plot of predicted versus computed binding energies for F–Cl complexes with the fourteen CN–R and the eight SiN–R molecules in Tables 1 and 3

series of complexes Cl–Cl···CN–R and Cl–Cl···SiN–R. The chlorine σ-hole in Cl–Cl has $V_{S,\max} = 23.8$ kcal/mol, considerably less positive than that of the chlorine in F–Cl.

The computed properties of the Cl–Cl···CN–R and Cl–Cl···SiN–R systems are in Table 4. Note that for the CN–R and SiN–R complexes with both F–Cl and Cl–Cl, the binding energy is always less with Cl–Cl than with F–Cl. Furthermore, all of the complexes, except for those with CN–Li and SiN–Li, have Cl–Cl, Cl–C and Cl–Si distances and BE values that are in the normal ranges for halogen bonds.

These observations underline the significance of the strong electric field of the F–Cl chlorine σ-hole in producing the high binding energies encountered in some of the complexes in Tables 1 and 3. When the ten BE in Table 4 are fit to the $\bar{I}_{S,\min}$ and $V_{S,\min}$ of the carbons and silicons, as per Eq. 4, the resulting relationship has $R^2 = 0.961$, RMS error $= 0.99$ kcal/mol and $F = 87$ (Table 2).

7 Discussion

The polarization/dative sharing interpretation of the deviations of many of the complexes in Tables 1 and 3 from typical halogen bonding is consistent with the results of another study by Del Bene et al. [39]. They found that the complexes of F–Cl with the bases NC–R (isomers of the CN–R molecules in Table 1) have, overall, quite normal halogen bonding features (see Table 5). Only F–Cl···NC–Li shows any tendency for a long F–Cl bond, a relatively short Cl–N separation and a high binding energy. Del Bene et al. attributed the differences between the F–Cl···CN–R and the F–Cl···NC–R complexes, at least in part, to the carbons being better electron donors. Our computed data in Table 5 quantify this explanation. While the $V_{S,\min}$ for NC–R and CN–R with the same R are quite similar, the nitrogen $\bar{I}_{S,\min}$ are 1.3–2.0 eV higher. Thus, the NC–R bases have a distinctly lesser propensity for strong polarization and dative sharing.

The important role of polarization is also brought out very emphatically by the fact that the silicon atoms in four of the SiN–R molecules in Tables 3 and 4—SiN–F, SiN–Cl, SiN–CCH and SiN–CCF—have *positive* $V_{S,\min}$. The electrostatic potentials on the surfaces of these silicons are totally positive. This might appear to preclude any attractive interactions with the positive σ-holes of the F–Cl and Cl–Cl chlorines. However, the silicon atom has a relatively high polarizability, and the electric fields of the σ-holes are presumably able to induce negative potentials on the silicons' surfaces with which the positive σ-holes can interact. It can be expected that dispersion also plays a role [21].

The plausibility of the polarization interpretation of the bonding in the F–Cl and Cl–Cl complexes of these four molecules can be demonstrated by using the formula [65],

$$\Delta E = -1/2\left(\alpha\varepsilon^2\right) \tag{5}$$

which gives the change in energy ΔE of the SiN–R molecule due to the electric field exerted along the Cl–Si axis by the chlorine σ-hole; α is the polarizability of the silicon along this axis. For this rough estimate, we use the polarizability of a free silicon atom, 5.38 Å^3 [64]. The electric field produced by F–Cl at a distance of 2.20 Å from the chlorine, corresponding to the complex with SiN–Cl and

Table 4 Computed properties for Cl–Cl···CN–R and Cl–Cl···SiN–R complexes

Complex	Properties of complex[a]			Properties of free CN-R, SiN-R[b]	
	R(Cl–Cl)[c]	R(Cl–C,Si)[d]	BE	$V_{S,\min}$	$\bar{I}_{S,\min}$
Cl–Cl···CN–F	2.010	2.896	3.13	−25.7	9.58
Cl–Cl···CN–Cl	2.013	2.831	3.71	−28.3	9.24
Cl–Cl···CN–H	2.014	2.837	3.73	−34.2	8.74
Cl–Cl···CN–CH_3	2.021	2.751	4.59	−39.5	8.25
Cl–Cl···CN–Li	2.524	1.662	14.97	−59.1	6.62
Cl–Cl···SiN–F	2.004	3.377	1.34	7.0	8.71
Cl–Cl···SiN–Cl	2.006	3.320	1.61	5.0	8.64
Cl–Cl···SiN–H	2.008	3.309	1.79	−2.9	8.49
Cl–Cl···SiN–CH_3	2.010	3.267	2.07	−6.0	8.14
Cl–Cl···SiN–Li	2.354	2.185	11.05	−26.3	6.72

[a] R(Cl–Cl) and R(Cl–C,Si) are distances in Å; BE is binding energy in kcal/mol. Computational level: MP2/aug'-cc-pVTZ

[b] $V_{S,\min}$, in kcal/mol, and $\bar{I}_{S,\min}$, in eV, refer to the carbons of the CN–R or the silicons of the SiN–R. Computational level: B3PW91/6-31G(d,p)

[c] Computed bond length in free Cl–Cl is 1.999 Å

[d] Sums of chlorine and carbon and chlorine and silicon van der Waals radii are 3.46 and 3.9 Å, respectively [36]

Table 5 Computed properties of complexes of F–Cl with a series of NC–R molecules

Complex	Properties of complex[a]			Properties of free base[b]	
	R(F–Cl)[c]	R(Cl–N)[d]	BE	$V_{S,\min}$	$\bar{I}_{S,\min}$
F–Cl···NC–NO_2	1.649	2.631	4.21	−18.4	11.97
F–Cl···NC–CN	1.650	2.608	4.51	−19.6	11.83
F–Cl···NC–CF_3	1.651	2.601	4.73	−25.0	11.37
F–Cl···NC–NC	1.651	2.596	4.73	−24.8	11.41
F–Cl···NC–F	1.653	2.578	5.32	−30.8	10.89
F–Cl···NC–H	1.656	2.541	5.49	−32.9	10.69
F–Cl···NC–Cl	1.656	2.536	5.92	−30.7	10.86
F–Cl···NC–CCH	1.657	2.520	6.08	−32.8	10.72
F–Cl···NC–CCF	1.658	2.515	6.20	−33.7	10.59
F–Cl···NC–CH_3	1.662	2.473	7.11	−39.6	10.06
F–Cl···NC–Li	1.697	2.263	11.81	−59.2	8.41

[a] R(F–Cl) and R(Cl–N) are distances in Å; BE is binding energy in kcal/mol. Computational level: MP2/aug'-cc-pVTZ. Data taken from reference [39]

[b] $V_{S,\min}$, in kcal/mol, and $\bar{I}_{S,\min}$, in eV, both refer to the nitrogen interacting with the chlorine. The positions of the $V_{S,\min}$ and the $\bar{I}_{S,\min}$ coincide; they are on the extensions of the C–N bonds. Computational level: B3PW91/6-31G(d,p)

[c] Computed bond length in free F–Cl is 1.639 Å

[d] Sum of chlorine and nitrogen van der Waals radii is 3.30 Å [36]

SiN–CCH (Table 3), is 0.0241 au = 1.24×10^{10} V/m [Gaussian 09 [56], B3PW91/6-31G(d,p)]. Then $\Delta E = -6.6$ kcal/mol. Considering that we did not use the actual polarizabilities of the silicons, the magnitude of this energy change ΔE is quite close to the computed binding energies of F–Cl with SiN–Cl and SiN–CCH (Table 3) and supports the polarization interpretation of these interactions. For the Cl–Cl complexes, in which the SiN–R silicon has a positive $V_{S,\min}$, ΔE will be smaller in magnitude (as are the binding energies) because the electric field is weaker, reflecting the less positive σ-hole of chlorine in Cl–Cl compared to F–Cl.

8 Summary

Complexes of F–Cl and Cl–Cl with CN–R and SiN–R molecules can exhibit a remarkable range of properties. These range from those of normal halogen bonds, mentioned earlier, to considerably higher binding energies, much shorter Cl–C and Cl–Si separations (approaching covalent bond lengths) and longer F–Cl and C–Cl distances.

We attribute these effects to the polarization of the CN–R carbons and the SiN–R silicons by the electric fields of the chlorine σ-holes. This polarization may merge into a degree of dative sharing of electrons by the carbons and silicons. Consistent with this interpretation is the fact that the departures from normal halogen bonding are more prevalent with F–Cl than with Cl–Cl; the former has a much more positive σ-hole and therefore a more polarizing electric field.

We prefer not to enter into a discussion of whether these stronger interactions should be labeled halogen bonds. What is significant is that the full range of binding energies of the complexes with either F–Cl or Cl–Cl can be represented analytically in terms of (a) the most negative electrostatic potentials $V_{S,\min}$ and (b) the lowest local ionization energies $\bar{I}_{S,\min}$ on the surfaces of the carbons and silicons. The $V_{S,\min}$ reflect the electrostatic interactions that are well established as a major driving force in normal halogen bonding, while the $\bar{I}_{S,\min}$ are measures of the polarizabilities and dative reactivities of the carbons and silicons. It is noteworthy that the marked variation in binding energies that is observed can be predicted from these properties of the free CN–R and SiN–R molecules *prior* to interaction.

We conclude by pointing out that halogen bonding is actually a subset of a broad group of noncovalent interactions. σ-Holes are not restricted to Group VII (halogens); they can also be found on covalently bonded atoms of Groups IV–VI, again on the extensions of the bonds to these atoms [12, 28, 29]. Thus, the Group IV, V and VI atoms can have four, three and two σ-holes, respectively (or more, if the atoms are hypervalent [66–68]). The magnitudes of the σ-hole potentials are governed by the same factors as apply for the halogens, and the atoms can interact directionally through positive σ-holes with negative sites. Noncovalent interactions between Group IV–VI atoms and Lewis bases have been known for decades, both experimentally and computationally [69–81]. Since 2007, it has been recognized that most of these are examples of σ-hole bonds [82–87]. We anticipate that polarization/dative

factors (in addition to electrostatic) can have similar effects for Groups IV–VI as for the halogens.

Acknowledgments We appreciate Dr. J. E. Del Bene's alerting us to the interesting results reported in references 35 and 39 and sending us preprints prior to their publication.

References

1. Brinck T, Murray JS, Politzer P (1992) Int J Quantum Chem 44(Suppl 19):55–64
2. Brinck T, Murray JS, Politzer P (1993) Int J Quantum Chem 48:73–88
3. Auffinger P, Hays FA, Westhof E, Shing Ho P (2004) Proc Natl Acad Sci USA 101:16789–16794
4. Stevens ED (1979) Mol Phys 37:27–45
5. Nyburg SC, Wong-Ng W (1979) Proc R Soc Lond Ser A 367:29–45
6. Ikuta S (1990) J Mol Struct (Theochem) 205:191–201
7. Price SL, Stone AJ, Lucas J, Rowland RS, Thornley AE (1994) J Am Chem Soc 116:4910–4918
8. Tsirelson VG, Zou PF, Tang T-H, Bader RWF (1995) Acta Crysta A 51:143–153
9. Lommerse JPM, Stone AJ, Taylor R, Allen FH (1996) J Am Chem Soc 118:3108–3116
10. Grabowski SJ, Bilewicz E (2006) Chem Phys Lett 427:51–55
11. Clark T, Henneman M, Murray JS, Politzer P (2007) J Mol Model 13:291–296
12. Politzer P, Murray JS, Clark T (2010) Phys Chem Chem Phys 12:7748–7757
13. Metrangolo P, Neukirch H, Pilati T, Resnati G (2005) Acc Chem Res 38:386–395
14. Politzer P, Lane P, Concha MC, Ma Y, Murray JS (2007) J Mol Model 13:305–311
15. Metrangolo P, Resnati G (eds) (2008) Halogen bonding: fundamentals and applications. Springer, Berlin
16. Di Paolo T, Sandorfy C (1974) Chem Phys Lett 26:466–469
17. Di Paolo T, Sandorfy C (1974) Can J Chem 52:3612–3622
18. Murray-Rust P, Motherwell WDS (1979) J Am Chem Soc 101:4374–4376
19. Murray-Rust P, Stallings WC, Monti CT, Preston RK, Glusker JP (1983) J Am Chem Soc 105:3206–3214
20. Ramasubbu N, Parthasarathy R, Murray-Rust P (1986) J Am Chem Soc 108:4308–4314
21. Riley KE, Murray JS, Concha MC, Politzer P, Hobza P (2009) J Chem Theor Comp 5:155–163
22. Shields ZP, Murray JS, Politzer P (2010) Int J Quantum Chem 110:2823–2832
23. Riley KE, Murray JS, Fanfrlík J, Řezáč J, Solá RJ, Concha MC, Ramos FM, Politzer P (2011) J Mol Model 17:3309–3318
24. Chopra D, Guru Row TN (2011) CrystEngComm 13:2175–2186
25. Metrangolo P, Murray JS, Pilati T, Resnati G, Politzer P, Terraneo G (2011) CrystEngComm 13:6593–6596
26. Metrangolo P, Murray JS, Pilati T, Resnati G, Politzer P, Terraneo G (2011) Cryst Growth Des 11:4238–4246
27. Politzer P, Murray JS, Concha MC (2008) J Mol Model 14:659–665
28. Politzer P, Murray JS (2009) In: Leszczynski J, Shukla M (eds) Practical aspects of computational chemistry. Springer, Heidelberg, pp 149–163
29. Murray JS, Riley KE, Politzer P, Clark T (2010) Aust J Chem 63:1598–1607
30. Hennemann M, Murray JS, Politzer P, Riley KE, Clark T (2011) J Mol Model. doi:10.1007/s00894-011-1263-5
31. Hermansson K (2002) J Phys Chem A 106:4695–4702
32. Qian W, Krimm S (2002) J Phys Chem A 106:6628–6636
33. Wang W, Wang N-B, Zheng W, Tian A (2004) J Phys Chem A 108:1799–1805
34. Murray JS, Concha MC, Lane P, Hobza P, Politzer P (2008) J Mol Model 14:699–704
35. Del Bene JE, Alkorta I, Elguero J (2010) J Phys Chem A 114:12958–12962
36. Bondi A (1964) J Phys Chem 64:441–451
37. Allen FH, Kennard O, Watson DG, Brammer L, Orpen AG, Taylor R (1987) J Chem Soc Perkin Trans II:S1–S19
38. Murray JS, Lane P, Clark T, Riley KE, Politzer P (2012) J Mol Model 18:541–548
39. Del Bene JE, Alkorta I, Elguero J (2011) Chem Phys Lett 508:6–9
40. Stewart RF (1979) Chem Phys Lett 65:335–342
41. Politzer P, Truhlar DG (eds) (1981) Chemical applications of atomic and molecular electrostatic potentials. Plenum Press, New York
42. Politzer P, Murray JS (2002) Theor Chem Acc 108:134–142
43. Murray JS, Politzer P (1998) J Mol Struct (Theochem) 425:107
44. Murray JS, Politzer P (2011) Wiley Interdisc Rev Comp Mol Sci 1:153–163
45. Bader RFW, Carroll MT, Cheeseman JR, Chang C (1987) J Am Chem Soc 109:7968–7979
46. Sjoberg P, Murray JS, Brinck T, Politzer P (1990) Can J Chem 68:1440–1443
47. Politzer P, Murray JS, Bulat FA (2010) J Mol Model 16:1731–1742
48. Koopmans TA (1934) Physica 1:104–113
49. Nesbet RK (1965) Adv Chem Phys 9:321–363
50. Politzer P, Abu-Awwad F, Murray JS (1998) Int J Quantum Chem 69:607–613
51. Politzer P, Shields ZPI, Bulat FA, Murray JS (2011) J Chem Theory Comp 7:377–384
52. Politzer P, Murray JS (2007) In: Toro-Labbé A (ed) Chemical reactivity, ch 8. Elsevier, Amsterdam, pp. 119–137
53. Jin P, Murray JS, Politzer P (2004) Int J Quantum Chem 96:394–401
54. Stott MJ, Zaremba E (1980) Phys Rev A 21:12–23
55. Vela A, Gázquez JL (1990) J Am Chem Soc 112:1490–1492
56. Frisch MJ, Trucks GW, Schlegel HB, Scuseria GE, Robb MA et al. (2009) Gaussian 09, Revision A.1. Gaussian Inc, Wallingford
57. Bulat FA, Toro-Labbé A, Brinck T, Murray JS, Politzer P (2010) J Mol Model 16:1679–1691
58. Politzer P, Murray JS, Concha MC (2002) Int J Quantum Chem 88:19–27
59. Murray JS, Peralta-Inga Z, Politzer P, Ekanayake K, LeBreton P (2001) Int J Quantum Chem Biophys Q 83:245–254
60. Haeberlein M, Murray JS, Brinck T, Politzer P (1992) Can J Chem 70:2209–2214
61. Gross KC, Seybold PG, Peralta-Inga Z, Murray JS, Politzer P (2001) J Org Chem 66:6919–6925
62. Ma Y, Gross KC, Hollingsworth CA, Seybold PG, Murray JS (2004) J Mol Model 10:235–239
63. Hintze J (2006) NCSS, PASS and GESS, Kaysville, UT (http://www.ncss.com)
64. Lide DR (ed) (2006) Handbook of chemistry and physics, 87th edn. CRC Press, Boca Raton
65. Bonin KD, Kresin VV (1997) Electric-dipole polarizabilities of atoms, molecules and clusters. World Scientific, Singapore
66. Clark T, Murray JS, Lane P, Politzer P (2008) J Mol Model 14:689–697
67. Murray JS, Lane P, Politzer P (2009) J Mol Model 15:723–729
68. O' Hair RAJ, Williams CM, Clark T (2010) J Mol Model 16:559–565

69. Miller DB, Sisler HH (1955) J Am Chem Soc 77:4998–5000
70. Kapecki JA, Baldwin JE (1969) J Am Chem Soc 91:1120–1123
71. Rosenfield RE Jr, Parthasarathy R, Dunitz JD (1977) J Am Chem Soc 99:4860–4862
72. Guru Row TN, Parthasarathy R (1981) J Am Chem Soc 103:477–479
73. Goldstein BM, Takusagawa F, Berman HM, Srivastava PC, Robins RK (1983) J Am Chem Soc 105:7416–7422
74. Burling FT, Goldstein BM (1992) J Am Chem Soc 114:2313–2320, and papers cited
75. Iwaoka M, Tomoda S (1996) J Am Chem Soc 118:8077–8084, and papers cited
76. Mitzel NW, Blake AJ, Rankin DWH (1997) J Am Chem Soc 119:4143–4148
77. Glusker JP (1998) Topics Curr Chem 198:1–56
78. Losehand U, Mitzel NW, Rankin DWH (1999) J Chem Soc Dalton Trans:4291–4297
79. Cozzolino AF, Vargas-Baca I, Mansour S, Mahmoudkhani AH (2005) J Am Chem Soc 127:3184–3190, and papers cited
80. Bleiholder C, Werz DB, Köppel H, Gleiter R (2006) J Am Chem Soc 128:2666–2674
81. Hagemann M, Mix A, Berger RJF, Pape T, Mitzel NW (2008) Inorg Chem 47:10554–10564
82. Murray JS, Lane P, Clark T, Politzer P (2007) J Mol Model 13:1033–1038
83. Murray JS, Lane P, Politzer P (2007) Int J Quantum Chem 107:2286–2292
84. Politzer P, Murray JS, Lane P (2007) Int J Quantum Chem 107:3046–3052
85. Murray JS, Lane P, Politzer P (2008) Int J Quantum Chem 108:2770–2781
86. Murray JS, Lane P, Nieder A, Klapötke TM, Politzer P (2010) Theor Chem Accts 127:345–354
87. Murray JS, Concha MC, Politzer P (2011) J Mol Model 17:2151–2157